ChemComm

RSC Publishing

COMMUNICATION

View Article Online
View Journal

Regioregular pyridyl[2,1,3]thiadiazole-*co*-indacenodithiophene conjugated polymers†

Cite this: DOI: 10.1039/c3cc43229g

Received 2nd May 2013,
Accepted 24th May 2013

DOI: 10.1039/c3cc43229g

www.rsc.org/chemcomm

Wen Wen,‡ Lei Ying,‡ Ben B. Y. Hsu, Yuan Zhang, Thuc-Quyen Nguyen and Guillermo C. Bazan*

Regioregular conjugated polymers containing alternating pyridyl[2,1,3]-thiadiazole (PT) and indacenodithiophene (IDT) structural units were synthesized. In these copolymers, the pyridyl nitrogen atoms on PT are precisely arranged along the backbone so that each one has an adjacent proximal and an adjacent distal counterpart across the two IDT flanking units. We find that despite the absence of obvious differences in orbital energy levels and optical bandgap, the regioregular materials exhibit larger charge carrier mobilities, as determined by using field effect transistor devices, and can yield higher solar cell power conversion efficiencies when mixed with fullerenes in bulk heterojunction active layers.

Bulk heterojunction (BHJ) solar cells based on conjugated polymers and fullerene acceptors have attracted much attention due to the possibility of solution fabrication.[1] This approach has led to power conversion efficiencies (PCE) of 8–10% based on the optimization of processing technologies and the development of new narrow band gap materials, primarily *via* the development of copolymers containing electron rich and electron poor fragments.[2] For conjugated polymers containing unsymmetric structural units, it is well-known that molecular structure, especially in terms of regioregularity, influences relevant optoelectronic properties. Classic examples include poly(3-alkylthiophene), poly(3-alkylthienylenevinylenes) and poly(2,5-bis(3-alkylthiophen-2-yl)thieno[3,2-*b*]thiophene).[3] We recently showed that by controlling the orientation of the pyridyl[2,1,3]-thiadiazole (PT) unit along the backbone vector one can obtain up to two orders of magnitude improvement in the carrier mobility, relative to counterparts that are not synthesized with specific control.[4] Moreover, these regioregular PT copolymers have been recently shown to be useful in the fabrication of field effect transistors (FETs) with hole mobilities of up to 6.7 $cm^2\ V^{-1}\ s^{-1}$.[5]

Indacenodithiophene (IDT), which contains two thiophene rings held in a rigid arrangement *via* a central phenyl ring, has been recently shown to be a suitable electron rich moiety for the design of narrow band gap conjugated polymers for incorporation into organic solar cells.[6] For the donor–acceptor (D–A) copolymer containing IDT and PT, it was found that in combination with [6,6]-phenyl-C_{71}-butyric acid methyl ester ($PC_{71}BM$) one could obtain PCEs on the order of 3.4%.[7] Based on the recent success in achieving high charge carrier mobilities discussed above, it seemed to be appropriate to consider how relevant basic physical properties and device function would be influenced by controlling the regiochemistry in PT–IDT copolymers; a structural consideration that has not received attention in the literature. In this contribution, we show that, indeed, regioregular IDT–PT copolymers show improved performances relative to regiorandom counterparts.

A two step procedure is required for the preparation of the regioregular polymer, see Scheme 1. First, the cross-coupling reaction of two equivalents of 4,7-dibromo-[1,2,5]thiadiazolo[3,4-*c*]pyridine ($PTBr_2$) with (4,4,9,9-tetrakis(4-hexylphenyl)-4,9-dihydro-*sec*-indaceno-[1,2-*b*:5,6-*b*′]dithiophene-2,7-diyl)bis(trimethylstannane) (**M1**) provided 4,4′-(4,4,9,9-tetrakis(4-hexylphenyl)-4,9-dihydro-*sec*-indaceno[1,2-*b*:5,6-*b*′]-dithiophene-2,7-diyl)bis(7-bromo-[1,2,5]thiadiazolo[3,4-*c*]pyridine) (**M2**). This reaction takes advantage of the higher reactivity of C–Br

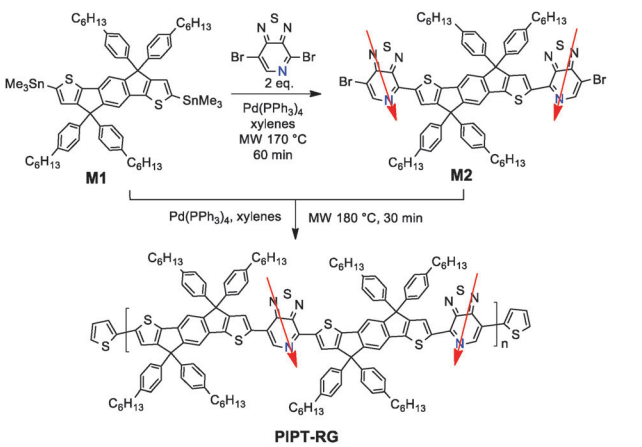

Scheme 1 Synthesis of **PIPT-RG**.

Center for Polymers and Organic Solids, Department of Chemistry and Biochemistry and Materials, University of California, Santa Barbara, California 93106-7150, USA. E-mail: bazan@chem.ucsb.edu

† Electronic supplementary information (ESI) available: Detailed synthesis of monomers and polymers, GPC, CV and DSC characteristics, detailed device fabrication and characterization including *J–V* curves and AFM images. See DOI: 10.1039/c3cc43229g

‡ Both authors contributed equally to this work.

adjacent to the pyridyl nitrogen on PT. In a second step, microwave-assisted Stille polymerization of **M1** with **M2** generates the target copolymer (**PIPT-RG**) with the regiochemistry as shown in Scheme 1. Specifically, for each PT unit one finds an adjacent distal PT (N atoms pointing away) and an adjacent proximal PT (N atoms pointing toward) fragments. Also for comparison with **PIPT-RG**, we prepared the IDT-*co*-PT copolymer *via* the established route reported in the literature in which one equivalent of $PTBr_2$ and one equivalent of the distannylated compound **M1** are subjected to Stille-coupling conditions.[7] The resulting product is expected to be less structurally precise and will be referred to as **PIPT-RA**.

Both **PIPT-RG** and **PIPT-RA** were end-capped after polymerization to remove unreacted bromide or trimethyltin end-groups,[8] and were purified by Soxhlet extraction using methanol, acetone, hexane and dichloromethane successively. The final polymers corresponded to the remaining chloroform soluble fraction. Gel permeation chromatography showed that the two polymers have very same molecular weight characteristics. The number average molecular weights are 60 kDa and 68 kDa for **PIPT-RA** and **PIPT-RG**, with polydispersities of 2.5 and 2.4, respectively (Fig. S1, ESI†). No noticeable phase transitions were observed for either material using differential scanning calorimetry up to 300 °C (Fig. S2, ESI†).

Fig. 1a shows the absorption profiles in the solid state. **PIPT-RA** exhibits a band centred at 710 nm, which corresponds to intermolecular charge transfer interactions between the donor and acceptor moieties. A higher energy transition is also observed at 417 nm, which has been previously assigned to a delocalized π–π* transition. These observations are consistent with properties described in the literature.[7] Fig. 1a also shows that **PIPT-RG** exhibits a nearly indistinguishable profile. From the onsets of absorption one can estimate the optical band gaps of the two copolymers to be nearly equal (1.60 eV). However, it is worth noting that the film absorption coefficient (α) of **PTPT-RA** (0.65×10^4 cm^{-1}) is smaller than that of **PIPT-RG** (0.77×10^4 cm^{-1}). This slightly stronger intensity is not understood at this point, but may be related to differences in the orientation of the polymer chains relative to the substrate surface or subtle differences in interchain packing, partly influenced by the regioregularity or the ordered vector of the PT unit along the polymer main chain.

Electrochemical measurements using cyclic voltammetry (CV) were carried out to estimate the orbital energy levels (Fig. S3, ESI†). The onsets of oxidation (E_{ox}) are determined to be 0.50 V and 0.45 V, corresponding to the highest occupied molecular orbital energy level (E_{HOMO}) of −5.30 eV and −5.25 eV for **PIPT-RA** and **PIPT-RG**, respectively. These values are similar to those reported in the literature and are equivalent given the errors in measurements and the assumptions in energy calculations.[7] It was also determined that nearly no difference in the HOMO values could be determined by using ultraviolet photoelectron spectroscopy (UPS) (Fig. 1b). The onsets of reduction (E_{red}) of the two copolymers were indistinguishable and located at approximately −1.20 V, corresponding to a lowest unoccupied molecular orbital energy (E_{LUMO}) of approximately −3.60 eV. Thus, the increase in regioregularity led to no detectable differences in energy levels as could be determined by conventional characterization methods.

To investigate charge transport properties of the polymers, bottom gate, bottom contact field effect transistors (FETs) with the architecture Si/SiO_2/DTS/polymer/Au were fabricated by spin-casting from 0.4 wt/v% of solution in 1,2-dichlorobenzene. Decyltrichlorosilane (DTS) was used as a dielectric passivation layer. Fig. 2 shows characteristic output and transfer curves after the films were thermally annealed at 150 °C for 10 minutes. From these data one obtains calculated hole mobilities of 0.2 cm^2 V^{-1} s^{-1} for **PIPT-RG** and 0.04 cm^2 V^{-1} s^{-1} for **PIPT-RA**. This result indicates that better charge carrier transport can be realized by controlling the regioregularity of **PIPT**, which is consistent with previously demonstrated better performance with other regioregular PT-containing polymers.[4]

Solar cells with an architecture described by ITO/molybdenum oxide (MoO_3)/polymer:$PC_{71}BM$/Al were fabricated as testing platforms, where the MoO_3 anode buffer layer was processed by spin-coating from aqueous MoO_3 solution.[9] We first screened device performance with different polymer/$PC_{71}BM$ weight ratios under AM 1.5 G solar irradiation at 100 mW cm^{-2} (Fig. S4 and Table S1, ESI†). The optimized weight ratio of the polymer to $PC_{71}BM$ was found to be 1 : 4 and PCEs of 3.4% for **PIPT-RA** (denoted as **A1** in Table 1) and 5.1% for **PIPT-RG** (denoted as **A2** in Table 1) were obtained by thermal annealing at 100 °C for 10 min,[10] respectively. Current density–voltage (*J*–*V*) characteristics are shown in Fig. 3, and the corresponding parameters are summarized in Table 1. Device **A2** exhibited higher shunt resistance (R_{sh} = 6.1 MΩ cm^{-2}) and lower series resistances (R_s = 0.66 KΩ cm^{-2}) than device **A1** (R_{sh} = 4.1 MΩ cm^{-2} and R_s = 1.23 KΩ cm^{-2}), respectively (Fig. S6, ESI†), indicating that the leakage current in **A2** is lower, and higher FF could be achieved.

We note here that topographic analysis using atomic force microscopy (AFM) shows that the **PIPT-RG**:$PC_{71}BM$ film is smoother (root mean square, rms, roughness of 0.5 nm) than **PIPT-RA**:$PC_{71}BM$ (rms = 3.5 nm). Furthermore, AFM also shows that **PIPT-RA**:$PC_{71}BM$ films exhibit round elevated features that suggest more pronounced BHJ phase separation. Even though the AFM images mainly reflect the surface of film morphologies, the relative suppression of domain

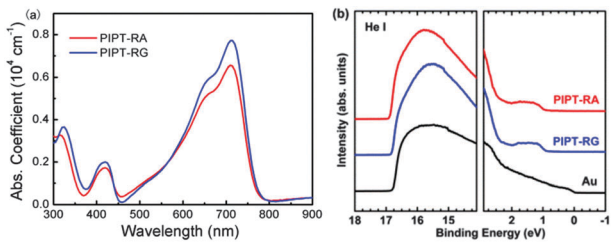

Fig. 1 UV-Vis absorption spectra (a) and UPS spectra (b) of **PIPT-RA** and **PIPT-RG** in the solid state.

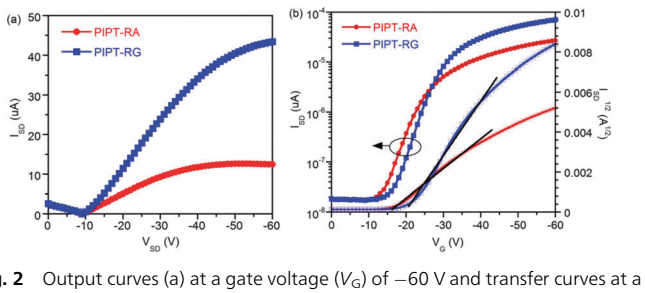

Fig. 2 Output curves (a) at a gate voltage (V_G) of −60 V and transfer curves at a source–drain voltage (V_{SD}) of −60 V (b) of films thermally annealed at 150 °C for 10 min.

Table 1 Summary of device properties

Device	Polymer:$PC_{71}BM$	V_{oc} (V)	J_{sc} (mA cm^{-2})	FF (%)	PCE (%)
A1	**PIPT-RA**:$PC_{71}BM$	0.82	10.5	40	3.4
A2	**PIPT-RG**:$PC_{71}BM$	0.88	12.1	48	5.1
B1	**PIPT-RA**:$PC_{71}BM$	0.86	12.3	43	4.5
B2	**PIPT-RG**:$PC_{71}BM$	0.88	13.9	55	6.7

Devices **A1** and **A2** have conventional structure: ITO/MoO_3/polymer:$PC_{71}BM$ (1 : 4 wt : wt)/Al, while **B1** and **B2** comprise the inverted structure: ITO/ZnO/polymer : $PC_{71}BM$ (1 : 4 wt : wt)/MoO_3/Ag.

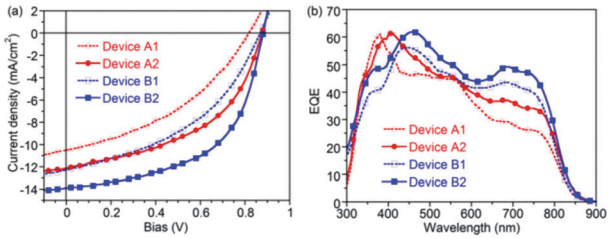

Fig. 3 *J–V* curves (a) and external quantum efficiency spectra (b) of devices based on polymer:$PC_{71}BM$.

size in **PIPT-RG**:$PC_{71}BM$ could be responsible for the improvements in device function.

Hole- and electron-only devices were specifically fabricated to estimate the charge mobilities of the blend films by a space charge limited current (SCLC) model as shown in Fig. S6 (ESI†). The electron mobility of two devices are comparable (2×10^{-4} cm^2 V^{-1} s^{-1}), most likely implying that the properties of the $PC_{71}BM$ pathway are not modified significantly. However, the **PIPT-RG**:$PC_{71}BM$ device exhibited higher hole mobility (1.3×10^{-4} cm^2 V^{-1} s^{-1}) relative to that of the **PIPT-RA**:$PC_{71}BM$ device (3.1×10^{-5} cm^2 V^{-1} s^{-1}). Since the collected current is dependent on the charge transporting properties of the BHJ layer, the higher hole mobility may be responsible for the larger J_{sc} observed for the **PIPT-RG** based device **A2**. Moreover, more balanced charge carrier mobility of **PIPT-RG**:$PC_{71}BM$ blends will lead to an improvement in FF.

Further optimization of solar cell performance was achieved through the use of inverted structures of the type ITO/ZnO/polymer : $PC_{71}BM$ (1 : 4 wt : wt)/MoO_3/Ag. These devices are denoted in Table 1 as **B1** and **B2**, respectively. Here the active layers were also annealed at 100 °C for 10 min before cathode deposition. The best inverted device structure (**B1**) with **PIPT-RA** provided a PCE of 4.5%, (J_{sc} = 12.13 mA cm^{-2}, V_{oc} = 0.86, and FF = 43%). The best performing device with **PIPT-RG** exhibited a much larger PCE of 6.7% (J_{sc} = 13.9 mA cm^{-2}, V_{oc} = 0.88 V and FF = 55%). The *J–V* characteristics and EQE spectra are shown in Fig. 3 and the device performances are summarized in Table 1. Note that the integrations of EQE spectra (Fig. 3b) are consistent with the J_{sc} results obtained from *J–V* measurements.

In conclusion, we have observed that the PCEs of indacenodithiophene-*co*-pyridyl[2,1,3]thiadiazole (IDT–PT) based copolymers can be improved by precisely controlling the orientation of the N-atom in the PT unit with respect to the polymer backbone. One finds that the optical and electrochemical properties of the regioregular **PIPT-RG** and the polymer obtained through conventional synthesis (**PIPT-RA**) are essentially identical within the certainties of the measurements. However, the FET hole mobility of **PIPT-RG** is higher than that of **PIPT-RA**. Of particular note is that the PCE values of BHJ solar cells with **PIPT-RG** are significantly improved and that in these devices one finds from single carrier diode measurements that the hole mobilities are also higher. With inverted device structures one can obtain with **PIPT-RG**:$PC_{71}BM$ a PCE of 6.7%. From a practical perspective, these findings highlight the benefits of controlling the regiochemistry of PT-containing narrow bandgap conjugated polymers.

We acknowledge the financial support from Mitsubishi Chemical Center for Advanced Materials (MC-CAM). We thank Prof. Alan J. Heeger, Dr Yanming Sun, Dr Soo-Hyung Choi and Dr Chan Luo for technical assistance and helpful discussions.

Notes and references

1 (*a*) Z. B. Henson, K. Mullen and G. C. Bazan, *Nat. Chem.*, 2012, **4**, 699–704; (*b*) J. W. Chen and Y. Cao, *Acc. Chem. Res.*, 2009, **42**, 1709–1718; (*c*) Y. J. Cheng, S. H. Yang and C. S. Hsu, *Chem. Rev.*, 2009, **109**, 5868–5923; (*d*) C. Li, M. Y. Liu, N. G. Pschirer, M. Baumgarten and K. Müllen, *Chem. Rev.*, 2010, **110**, 6817–6855.
2 (*a*) J. You, L. Dou, K. Yoshimura, T. Kato, K. Ohya, T. Moriarty, K. Emery, C. C. Chen, J. Gao, G. Li and Y. Yang, *Nat. Commun.*, 2013, **4**, 1–10; (*b*) Z. He, C. Zhong, S. Su, M. Xu, H. Wu and Y. Cao, *Nat. Photonics*, 2012, **6**, 593–597; (*c*) C. Cabanetos, A. El Labban, J. A. Bartelt, J. D. Douglas, W. R. Mateker, J. M. J. Fréchet, M. D. McGehee and P. M. Beaujuge, *J. Am. Chem. Soc.*, 2013, **135**, 4656–4659; (*d*) Y. Huang, X. Guo, F. Liu, L. J. Huo, Y. N. Chen, T. P. Russell, C. C. Han, Y. F. Li and J. H. Hou, *Adv. Mater.*, 2012, **24**, 3383–3389; (*e*) T. B. Yang, M. Wang, C. H. Duan, X. W. Hu, L. Huang, J. B. Peng, F. Huang and X. Gong, *Energy Environ. Sci.*, 2012, **5**, 8208–8214.
3 (*a*) I. Osaka and R. D. McCullough, *Acc. Chem. Res.*, 2008, **41**, 1202–1214; (*b*) R. S. Loewe and R. D. McCullough, *Chem. Mater.*, 2000, **12**, 3214–3221; (*c*) I. McCulloch, M. Heeney, C. Bailey, K. Genevicius, I. MacDonald, M. Shkunov, D. Sparrowe, S. Tierney, R. Wagner, W. Zhang, M. L. Chabinyc, R. J. Kline, M. D. McGehee and M. F. Toney, *Nat. Mater.*, 2006, **5**, 328–333.
4 L. Ying, B. B. Y. Hsu, H. M. Zhan, G. C. Welch, P. Zalar, L. A. Perez, E. J. Kramer, T. Q. Nguyen, A. J. Heeger, W. Y. Wong and G. C. Bazan, *J. Am. Chem. Soc.*, 2011, **133**, 18538–18541.
5 H. R. Tseng, L. Ying, B. B. Y. Hsu, L. A. Perez, C. J. Takacs, G. C. Bazan and A. J. Heeger, *Nano Lett.*, 2012, **12**, 6353–6357.
6 (*a*) I. McCulloch, R. S. Ashraf, L. Biniek, H. Bronstein, C. Combe, J. E. Donaghey, D. I. James, C. B. Nielsen, B. C. Schroeder and W. Zhang, *Acc. Chem. Res.*, 2012, **45**, 714–722; (*b*) Y. Zhang, J. Zou, H. L. Yip, K. S. Chen, J. A. Davies, Y. Sun and A. K. Y. Jen, *Macromolecules*, 2011, **44**, 4752–4758; (*c*) W. Zhang, J. Smith, S. E. Watkins, R. Gysel, M. McGehee, A. Salleo, J. Kirkpatrick, S. Ashraf, T. Anthopoulos, M. Heeney and I. McCulloch, *J. Am. Chem. Soc.*, 2010, **132**, 11437–11439; (*d*) K. S. Chen, Y. Zhang, H. L. Yip, Y. Sun, J. A. Davies, C. Ting, C. P. Chen and A. K. Y. Jen, *Org. Electron.*, 2011, **12**, 794–801; (*e*) Y. C. Chen, C. Y. Yu, Y. L. Fan, L. I. Hung, C. P. Chen and C. Ting, *Chem. Commun.*, 2010, **46**, 6503–6505; (*f*) C. P. Chen, S. H. Chan, T. C. Chao, C. Ting and B. T. Ko, *J. Am. Chem. Soc.*, 2008, **130**, 12828–12833.
7 Y. Sun, S. C. Chien, H. L. Yip, Y. Zhang, K. S. Chen, D. F. Zeigler, F. C. Chen, B. P. Lin and A. K. Y. Jen, *J. Mater. Chem.*, 2011, **21**, 13247–13255.
8 J. K. Park, J. Jo, J. H. Seo, J. S. Moon, Y. D. Park, K. Lee, A. J. Heeger and G. C. Bazan, *Adv. Mater.*, 2011, **23**, 2430–2435.
9 (*a*) F. M. Liu, S. Y. Shao, X. Y. Guo, Y. Zhao and Z. Y. Xie, *Sol. Energy Mater. Sol. Cells*, 2010, **94**, 842–845; (*b*) S. Murase and Y. Yang, *Adv. Mater.*, 2012, **24**, 2459–2462.
10 G. Li, V. Shrotriya, J. S. Huang, Y. Yao, T. Moriarty, K. Emery and Y. Yang, *Nat. Mater.*, 2005, **4**, 864–868.